Reptational dynamics in dissipative particle dynamics simulations of polymer melts

Petri Nikunen
CSC-Scientific Computing Ltd., P.O. Box 405, FI-02101 Espoo, Finland

Ilpo Vattulainen*
Laboratory of Physics and Helsinki Institute of Physics, Helsinki University of Technology, Espoo, Finland; MEMPHYS-Center for Biomembrane Physics, University of Southern Denmark, Odense, Denmark; and Institute of Physics, Tampere University of Technology, Tampere, Finland

Mikko Karttunen†
Department of Applied Mathematics, The University of Western Ontario, London, Ontario, Canada
(Received 12 December 2005; revised manuscript received 6 February 2007; published 30 March 2007)

Understanding the fundamental properties of polymeric liquids remains a challenge in materials science and soft matter physics. Here, we present a simple and computationally efficient criterion for topological constraints, i.e., uncrossability of chains, in polymeric liquids using the dissipative particle dynamics (DPD) method. No new length scales or forces are added. To demonstrate that this approach really prevents chain crossings, we study a melt of linear homopolymers. We show that for short chains the model correctly reproduces Rouse-like dynamics whereas for longer chains the dynamics becomes reptational as the chain length is increased—something that is not attainable using standard DPD or other coarse-grained soft potential methods.

DOI: 10.1103/PhysRevE.75.036713 PACS number(s): 02.70.−c, 61.25.Hq, 82.20.Wt, 87.15.Aa

I. INTRODUCTION

The static and dynamic properties of polymeric liquids are, by and large, dominated by topological constraints. The origin of these constraints is easy to understand: polymers can slide past but not penetrate through each other. That is the physical origin of the reptation model [1–3] which is the most successful theory in describing the behavior of entangled polymers. Despite active research in the field, entangled polymeric liquids keep posing many challenges to theorists [4–6], experimentalists [7–9], and computational modelers [10–16]. The importance of understanding the fundamentals of polymeric liquids can hardly be overemphasized as they are one of the key issues in novel (bio)materials science [17,18].

The dynamics of polymer melts is typically described in terms of the Rouse and reptation models [3]. Short chains are able to move to any direction and are not entangled. That is the physical origin of the Rouse model [3,19]. For longer chains, entanglements and uncrossability of chains cannot be ignored, and the chains become constrained to move in the direction of the chain backbone. This motion resembles that of a reptating snake—hence the name reptation model [1–3].

Computer simulations offer a detailed look into polymers and their dynamics. In classical molecular-dynamics simulations the system size and simulation time pose limits as they are typically of the order of 10 nm in linear size and around 10 ns in time. In contrast, coarse grained methods, such as dissipative particle dynamics (DPD), allow access to micrometer and microsecond scales, see, e.g., Ref. [20]. That is due to the soft potentials, and, like everything in life, they do not come without a price to pay: the softness of the conservative potentials allows the chains to slide through each other. This is unphysical since in nature polymers are uncrossable.

The fact that polymers can penetrate through themselves in DPD simulations affects the dynamics of the system. A direct consequence of this is that the scaling laws obtained from DPD simulations of polymer melts [21,22] are not able to describe entangled liquids. Whereas that is not a problem in studying the equilibrium properties in the Rouse regime, reptation cannot be studied using the basic DPD model with soft interactions.

To preserve the advantages of coarse-grained models and to correct for their deficiencies, Padding and Briels [13] recently introduced an algorithm that explicitly detects and prevents bond crossings. They consider bonds as elastic bands that become entangled and use energy minimization to determine the entanglement positions. This approach is general and very promising but it is also somewhat complicated to implement and computationally intensive [13]. To demonstrate their approach, Padding and Briels [13,23] studied a melt of linear homopolymers, and showed that the system indeed exhibits reptation dynamics.

Another promising approach was put forward by Pan and Manke [24]. They reduce the frequency of bond crossings by introducing segmental repulsive forces between the points of nearest contact between neighboring chains. This approach is simple to implement but the introduction of a new force and a related cutoff increases the computational load, and adds a new length scale whose physical determination is somewhat ambiguous. On the other hand, the model seems to be able to capture both the Rouse and reptational behavior [24] like that of Padding and Briels [13,23].

*Email address: vattulai@csc.fi
†URL: www.softsimu.org. Email address: mkarttu@uwo.ca

It is also possible to make polymers uncrossable by tuning the conservative forces within polymer chains. Indeed, if a certain geometric criterion is met, then it is impossible for polymer chains to cross. In the case of hard interparticle potentials, such as the Lennard-Jones potential, this criterion is easy to satisfy because hard potentials have radii within which other particles cannot penetrate. Soft potentials do not have such radii. Therefore the polymer models used in DPD must be constructed with care.

In this paper, we introduce a simple and generic criterion based on simple geometrical arguments to solve the crossability problem. No new forces are added, the approach is conceptually simple and does not depend on the level of coarse graining. Importantly, it allows easy, and if necessary even on-the-fly, tuning between the Rouse and reptation regimes. As a test, we carry out extensive DPD simulations for polymer melts. We demonstrate that if the geometric criterion mentioned above is satisfied, the system exhibits Rouse-like behavior for short chains and reptational dynamics for longer chains. If the criterion is not satisfied, in turn, the dynamics is Rouse-like for all chain lengths.

Besides its applicability for studies of polymer melts, the present approach is expected to be useful also in DPD, and other coarse-grained simulations of biomolecular systems such as lipid membranes especially in connection with constant pressure simulations, see Refs. [25,26] and references therein. For example, the use of soft DPD interactions (i.e., interpenetrable particles) and the consequent lack of entanglement effects renders the lateral diffusion of lipids in membranes somewhat unphysical. The idea proposed here allows one to get rid of these problems to a large degree yet still retaining the coarse-grained nature of the system.

The rest of this paper is organized as follows. In the next section we will briefly describe the DPD method. Section III describes the criterion for including topological constraints in DPD, or for that matter any other soft potential, simulation. In Sec. V we show results from our simulations and compare them to other methods. Finally, we finish with a discussion and outlook in Sec. VI.

II. DISSIPATIVE PARTICLE DYNAMICS

In DPD, the time evolution of particles is given by the Newton's equations of motion, and the total force acting on particle i is given as a sum of pairwise conservative, dissipative, and random forces, respectively, as $\vec{F}_i=\Sigma_{i\neq j}(\vec{F}_{ij}^C+\vec{F}_{ij}^D+\vec{F}_{ij}^R)$.

The conservative force is independent of the dissipative and random forces. Typically it takes the form

$$\vec{F}_{ij}^C=\begin{cases} a_{ij}(1-r_{ij}/r_c)\vec{e}_{ij} & \text{if } r_{ij}<r_c \\ 0 & \text{otherwise,} \end{cases} \tag{1}$$

with $\vec{r}_{ij}\equiv\vec{r}_i-\vec{r}_j$, $r_{ij}\equiv|\vec{r}_{ij}|$, and $\vec{e}_{ij}\equiv\vec{r}_{ij}/r_{ij}$. The variable a_{ij} describes the repulsion between particles i and j, and thus produces excluded volume interactions.

The dissipative force is expressed as

$$\vec{F}_{ij}^D=-\gamma\omega^D(r_{ij})(\vec{v}_{ij}\cdot\vec{e}_{ij})\vec{e}_{ij}, \tag{2}$$

where γ is a friction parameter, $\omega^D(r_{ij})$ is a weight function for the dissipative force, and $\vec{v}_{ij}\equiv\vec{v}_i-\vec{v}_j$. The dissipative force slows down the particles by decreasing kinetic energy from them. This effect is balanced by the random force due to thermal fluctuations,

$$\vec{F}_{ij}^R=\sigma\omega^R(r_{ij})\zeta_{ij}\vec{e}_{ij}, \tag{3}$$

where σ is the amplitude of thermal noise, $\omega^R(r_{ij})$ is the weight function for the random force, and $\zeta_{ij}(t)$ are Gaussian random variables with $\langle\zeta_{ij}(t)\rangle=0$ and $\langle\zeta_{ij}(t)\zeta_{kl}(t')\rangle=(\delta_{ik}\delta_{jl}+\delta_{il}\delta_{jk})\delta(t-t')$. The condition $\zeta_{ij}(t)=\zeta_{ji}(t)$ is required for momentum conservation. That is a necessary condition for the inclusion of hydrodynamic interactions.

The weight functions $\omega^D(r_{ij})$ and $\omega^R(r_{ij})$ cannot be chosen arbitrarily. Español and Warren [27] showed that the fluctuation-dissipation relations $\omega^D(r_{ij})=[\omega^R(r_{ij})]^2$ and $\sigma^2=2\gamma k_BT$ must be satisfied for the system to have a canonical equilibrium distribution. Here T is the temperature of the system and k_B is the Boltzmann constant. The functional form of the weight functions is not defined by the DPD method but virtually all DPD studies use

$$\omega^D(r_{ij})=[\omega^R(r_{ij})]^2=\begin{cases}(1-r_{ij}/r_c)^2 & \text{if } r_{ij}<r_c \\ 0 & \text{otherwise.}\end{cases} \tag{4}$$

Coarse graining in DPD comes in through the soft conservative potential and forces [Eq. (1)]. Yet also other interactions can be derived through systematic coarse-graining procedures, for example, see Refs. [28–31]. A detailed account of DPD, derivation of time and length scales, and its applications is given by Groot [20]. An in-depth discussion of coarse graining by Español can be found in the same reference.

III. TOPOLOGICAL CONSTRAINTS

To take into account the topological constraints, chain crossings must be prevented. As discussed in the introduction, there are currently two off-lattice methods [13,24] for this purpose. It is also possible to make polymers uncrossable by tuning the conservative forces within polymer chains. Here, we give general directions how to do this.

First, each individual bead has a radius $r_{\min}/2$ which is impenetrable to other beads. In systems with Lennard-Jones potentials that condition is automatically satisfied due to the r^{-12} part that takes care of the Fermi exclusion principle. In mesoscopic simulations with soft potentials that constraint needs special attention. Second, the intramolecular bonds have some maximum stretch, $\ell_{\max}$. By using simple geometry, we can postulate that if the condition

$$\sqrt{2}r_{\min}>\ell_{\max} \tag{5}$$

is satisfied, any two bonds cannot cross each other, see Fig. 1. The length scales involved, i.e., $r_{\min}$ and $\ell_{\max}$, have a clear physical meaning.

The obvious question is how to satisfy Eq. (5). As an example, let us consider DPD simulations of polymers. The

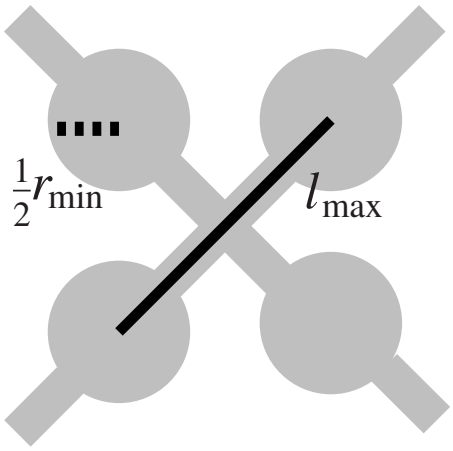

FIG. 1. Two bonds crossing each other. If Eq. (5) is satisfied, crossings cannot occur.

parameters used in these simulations are often justified on the basis of the Flory-Huggins theory [20,32], where the key component is the solubility as expressed by the χ parameters. Then, in simulations of block co-polymers, e.g., it is the mutual repulsion between the different components that matters—as a matter of fact, the values of the interaction parameters a_{ij} may be derived in different ways and their values tell only about the degree of coarse graining. The condition set by Eq. (5) can thus be met by a proper degree of coarse graining, complemented by a reasonable description for bond stretching (springs). Indeed, $\ell_{\max}$ is limited by the type of springs used in the model. With finitely extendable nonlinear elastic (FENE) springs [33] that is easy to tune as they have only finite extension after which the force becomes infinite. With harmonic springs more care is needed to satisfy Eq. (5) as there is no FENE-like cutoff present. We will return to that in Sec. V.

IV. SIMULATIONS

For simplicity, and to be able to compare the model with other simulations, we considered a melt of linear polymers in a cubic box (three dimensional) with periodic boundary conditions. To avoid finite-size effects, the linear box size L was chosen to be at least 1.75 times the average end-to-end distance of chains. We also carried out simulations with different box sizes to ensure that the systems were free of finite-size effects. That was done since it is known that static properties are affected by them [34]. The results were the same within statistical error.

All the systems had 128 chains consisting of N monomers, and no additional solvent or free monomers were present. All monomers were chosen to be identical, and thus the monomer mass was set equal to unity, $m=1$, fixing the scale of mass. The cutoff distance r_c sets the length scale for the model. The conservative forces had the form given in Eq. (1), with $r_c=1$ and $a_{ij}=a$ for all particle pairs. The values of a, as well as other simulation parameters used in these simulations, are listed in Table I.

For the random and dissipative forces we used Eqs. (2) and (3) with the common choices [20,32,35,36] $\gamma=4.5$ and $\sigma=3$. This sets the temperature to $k_BT=1$, and hence the time scale is given by $\sqrt{mr_c^2/k_BT}$.

TABLE I. The parameters used in this study.

a (amplitude of the conservative force)	50	100	150	200
k (spring constant)	100	200	300	400
Δt (time step)	0.03	0.02	0.015	0.0125

The monomers were connected using harmonic springs, i.e., $\vec{F}_i^S=\Sigma_j k(\ell-r_{ij})\vec{e}_{ij}$, where the sum runs over all particles j to which particle i is connected. The equilibrium bond length was set to $\ell=0.95$. That particular value was chosen as it is very near the first maximum of the radial distribution function (at the density $\rho=1$). The spring constant was chosen to be $k=2a$. If k is much smaller, bonds are very flexible and Eq. (5) is not satisfied. On the other hand, if k is much larger than a, the time step Δt must be decreased from the value set by the choice of a thus decreasing the computational efficiency. Another possibility would be to use FENE springs [34] since they have finite extension.

The density was chosen to be $\rho=1$, which is lower than the densities typically used in DPD simulations [20,32]. The reason for high densities is to give different repulsive interactions for different particle types. This works only if particles overlap each other considerably. In the present work, we do not need such interactions, and therefore the lower density is sufficient. In fact, the density of $\rho=1$ sets the monomer-monomer coordination number near 12, which is a typical value for real liquids.

All systems were started from random flight initial configurations and they were equilibrated for 10^6 time steps. After the equilibration, we simulated systems at least for 10^7 time steps to compute the desired quantities. Equations of motion were integrated using the DPD-VV (velocity Verlet) algorithm [35,37,38].

V. RESULTS

Figure 2 shows snapshots of the chain motion during the simulation at different times and regimes. For clarity, the chain is projected onto two dimensions. It is immediately clear that the motions in Figs. 2(a) and 2(b) are qualitatively different. Figure 2(a) shows Rouse-like motion in which the polymers are free to move in every direction, and Fig. 2(b) represents reptation confined into a tube.

The term "Rouse-like motion" here refers to the unentangled motion in order to distinguish it from the reptational motion. It is important to note here that the model applied in the current work is a stiff spring model resembling a freely jointed chain model, not the classical bead and spring model of Rouse.

A. Radial distribution function

We will now study the static properties to see the effect of Eq. (5). As discussed, by tuning the chain stiffness it is possible to move gradually from the Rouse regime to reptation.

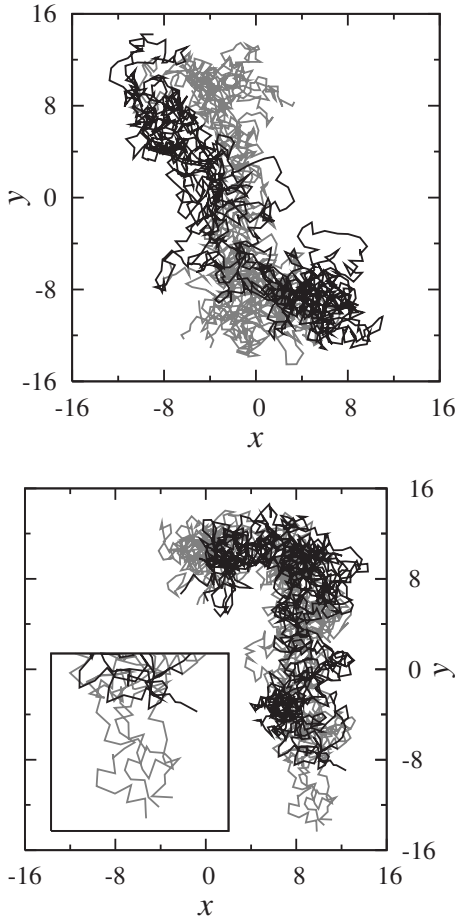

FIG. 2. The snapshots present ten superpositions of configurations for a chain of length $N=256$ taken at times 100 apart. Gray: times up to 500 (in DPD time units); black: times from 500 to 1000. (a) Rouse dynamics ($a=25$, $k=50$) and (b) reptation ($a=100$, $k=200$).

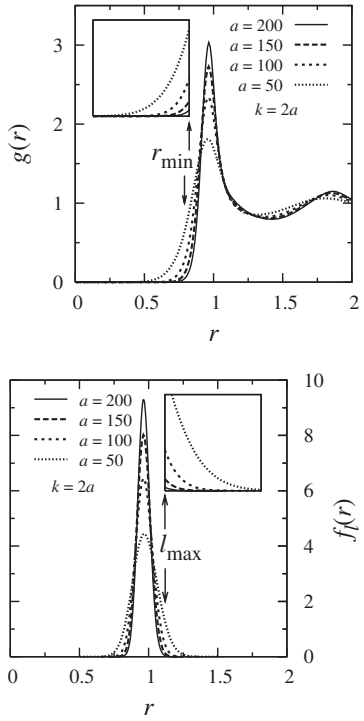

FIG. 3. (a) Radial distribution function in the case of $N=256$. The arrow shows the distance $r_{\min}$, and the inset shows the region at lengths shorter than $r_{\min}$. As seen in the figure, the condition is well fulfilled for the largest a. As the parameter a becomes smaller, the deviations grow. (b) Bond-length distribution ($N=256$). The inset shows the region at values larger than $\ell_{\max}$. The arrows show a set of $r_{\min}$ and $\ell_{\max}$ values that satisfy Eq. (5) in the case $a=200$.

This should be reflected in both the radial distribution function and the bond-length distribution.

The radial distribution function (RDF) $g(r)$ describes the qualitative structure of a fluid. It is defined as $g(r)=\rho(r)/\rho$ where $\rho(r)$ is the average density from a given particle at a distance r. Figures 3(a) and 3(b) show the radial distribution function $g(r)$ and the bond-length distribution $f_\ell(r)$ for different parameter sets for chains of length $N=256$. The arrows in the figures indicate the set of values of $r_{\min}$ and $\ell_{\max}$ that satisfy Eq. (5) for the largest value of a ($a=200$). As the insets indicate, the condition starts to become violated at small values of a. As the figures show, Eq. (5) is satisfied for larger values of a and k. The very small nonzero values below $r_{\min}$ for $a=200$ are due to the softness of the interparticle DPD potentials.

The above can be characterized by taking a look at the average bond lengths and their mean-square deviations. For $a_{ij}=50$ we measured $\langle\ell\rangle=0.977\pm0.091$. As the strength of interaction is increased we obtain $\langle\ell\rangle=0.969\pm0.063$ for $a_{ij}=100$, $\langle\ell\rangle=0.966\pm0.051$ for $a_{ij}=150$, and $\langle\ell\rangle=0.96\pm0.044$ for $a_{ij}=200$. The most important issue is the decrease of the mean-square deviation as that restricts the amount of overlap between the monomers of different chains. Importantly, for FENE chains this can be directly controlled by using the above measurements and RDF as a guideline and setting the maximum extent of the chain to an appropriate value.

A comparison of the radial distribution functions shows that the current approach allows for tuning between typical DPD results [22,32,38] and typical molecular-dynamics simulations using Lennard-Jones (LJ) potentials [34]. As the bond strength is increased ($a\geqslant100$, $k\geqslant200$), $g(r)$ becomes qualitatively similar to that from a LJ system.

Let us close this discussion by the following note about the choice of the geometric criterion: Here, we used an operational definition and chose 0.05 as the value (see Table II for the values of $r_{\min}$ and $\ell_{\min}$ for different a_{ij} satisfying the chosen criterion). It is also possible to try to fit the small values of $g(r)$ to a curve and extrapolate to the value at which $g(r)=0$. Whether or not that is a feasible approach

TABLE II. The values of $r_{\min}$ and $\ell_{\min}$ for different a_{ij} when using the operative criterion 0.05.

a_{ij}	$r_{\min}$	$\ell_{\min}$
50	0.598	1.266
100	0.712	1.177
150	0.763	1.138
200	0.793	1.115

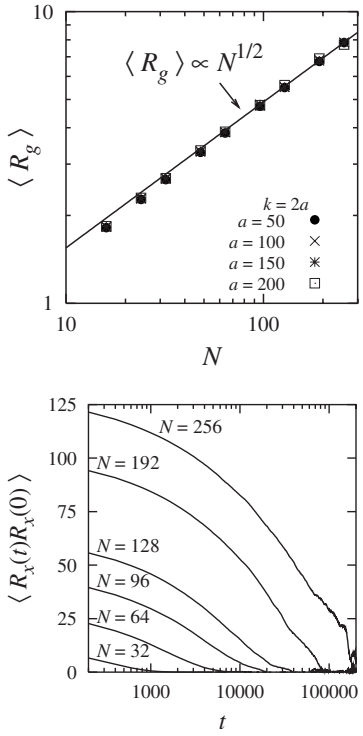

FIG. 4. (a) The radius of gyration as a function of chain length for different parameters. (b) The end-to-end vector autocorrelation ($a=100$, $k=200$) for chains of different length.

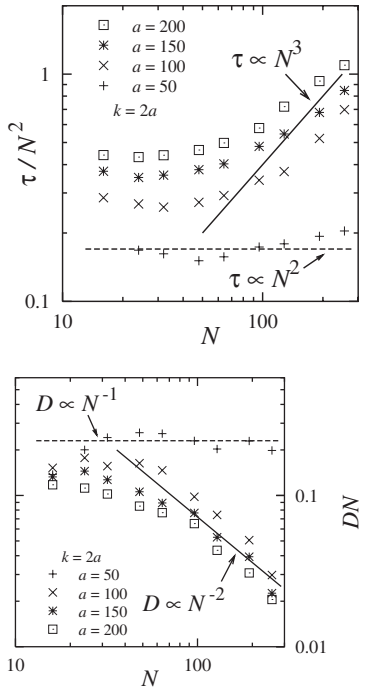

FIG. 5. (a) Scaling of the longest relaxation time τ. There is a crossover from Rouse scaling ($\tau \propto N^2$) to reptation ($\tau \propto N^3$). (b) Similarly, the proper scaling limits are reached for the diffusion coefficient D.

depends on softness of the potentials as $g(r)$ may approach zero very slowly. Our operational choice is a conservative one and guarantees correct behavior.

B. Static scaling

Next, we studied the end-to-end distance R and the radius of gyration R_g. The former is defined as $R=|\vec{R}|=|\vec{r}_1-\vec{r}_N|$ and the latter as $R_g^2=\frac{1}{N}\Sigma_{i=1}^{N}(\vec{r}_i-\vec{r}_{\rm cm})^2$, where $\vec{r}_{\rm cm}=\frac{1}{N}\Sigma_{i=1}^{N}\vec{r}_i$. In a polymer melt, they are expected to scale as $\langle R\rangle \propto N^{1/2}$ and $\langle R_g\rangle \propto N^{1/2}$ in both Rouse and the reptation regime. Previous studies using soft potentials [21] and systems with more realistic hard potentials [34] exhibit scaling. In Fig. 4(a) we plot the results for the radius of gyration for different parameter sets. It is clear from the figure that the system exhibits the proper scaling behavior independently of the interaction parameters as it should.

C. Relaxation time

One of the main practical obstacles in simulations of polymeric solutions is the long stress relaxation time. The longest relaxation time τ depends on the molecular weight and the reptation theory predicts it to scale as $\tau \propto N^3$. That prediction assumes only one mechanism for relaxation, i.e., diffusion along the contour [1]. The Rouse model predicts a distinctly different behavior with $\tau \propto N^2$.

To estimate the scaling behavior, we measured the end-to-end autocorrelation function. It is shown in Fig. 4(b) for polymers of different length. Assuming exponential decay, i.e.,

$$\langle \vec{R}(t)\cdot\vec{R}(0)\rangle \sim \exp(-t/\tau),$$

we can extract the longest relaxation time τ by fitting. Figure 5(a) shows that both scaling regimes are captured properly. Figure 5(a) illustrates one of the main results of this paper: the simple criterion set by Eq. (5) allows an easy, physical, and computationally efficient tuning between the Rouse regime and reptation.

The scaling exponents 2 and 3 for Rouse and reptation, in respective order, are the limiting laws. The exponents have been frequently debated in the literature. For example, in the entangled regime, Padding and Briels [23] found two scaling regimes in τ, one with exponent 2.8 and the other one with exponent 3.5. The dependence $\tau \propto N^{3.4}$ is experimentally observed for the longest relaxation time in the entangled regime [39]. This discrepancy is often associated with fluctuations of the contour length of the primitive path. In a real situation, however, the tube has a characteristic lifetime and the length of the primitive path fluctuates since the Rouse modes continue in the direction along the primitive path. The presence of fluctuations reduces the lifetime of the initial tube, i.e., the maximum relaxation time τ, for which reason the apparent scaling exponent is higher than 3 when N is finite. The true asymptotic behavior $\tau \propto N^3$ should still hold as $N \to \infty$.

Determining the value of the exponent was not the main goal here, and thus we did not attempt to evaluate it in a high precision—we will focus on that in a future publication. The above simply demonstrates that it is indeed possible to include topological constraints in the soft DPD model realistically without introducing additional length scales and forces.

D. Diffusion

The motion of a polymer, or its segments, is described by the diffusion coefficient. Typically, one measures the center-of-mass diffusion coefficient for a polymer chain, i.e.,

$$D = \lim_{t\to\infty} \frac{1}{6t}\langle[\vec{r}_{\mathrm{cm}}(t) - \vec{r}_{\mathrm{cm}}(0)]^2\rangle.$$

The scaling of D with molecular weight has been studied intensely over the years, see, e.g., the discussion in [4].

The theory predicts two scaling limits, $D \propto N^{-1}$ for the Rouse model and $D \propto N^{-2}$ for the pure reptation model (N is proportional to molecular weight). Figure 5(b) shows that both scaling regimes are found.

Considering the nature of the DPD model, it is remarkable that both regimes are recovered. In simulations using the plain DPD model without paying attention to the criterion given by Eq. (5), only Rouse scaling has been observed [21,22] even in the case of long polymers.

As with the longest relaxation time, the exponents typically reported are between the scaling limits. Pearson *et al.* [40] measured D as a function of molecular weight M_w in polyethylene and they found that the diffusion coefficient follows a power law $D=1.65M_w^{-1.98}\mathrm{cm}^2/\mathrm{s}$ for the entire range from $M_w=600$ to $M_w=12000$ (g/mol). The simulations by Kremer and co-workers [11,34] and Padding and Briels [13,23] confirmed this finding: the center-of-mass diffusion coefficient scales as $D \propto N^{-2}$ in melt.

Padding and Briels [23] compared their results to different simulations and experiments, and found that in ethylene the crossover between Rouse-like and reptational dynamics takes place at molecular weight of 560 g/mol (which corresponds to 40 ethylenes). Because in Fig. 5(b) the crossover takes place between $N=40$ and $N=60$, we can picture each particle roughly as one ethylene unit.

VI. DISCUSSION

In this paper we have provided directions for how to construct a polymer model such that one can be sure that polymer chains are uncrossable. No new forces or length scales were added. To demonstrate that this approach really prevents chain crossings, we have carried out extensive DPD simulations for polymer melts. We showed that if the criterion set by Eq. (5) is satisfied, the system exhibits Rouse-like behavior for short chains and reptational dynamics for longer chains. If the criterion is not satisfied, in turn, the dynamics is Rouse-like for all chain lengths. This approach can also be used for systems of, e.g., block co-polymers with different interactions and monomer sizes, and shear simulations. In practice, one can always run a short test simulation, and use $g(r)$ and the bond length distribution [as in Figs. 3(a) and 3(b)] to verify that the criterion set by Eq. (5) is met.

There is one other issue that we need to address, namely by tuning the chain stiffness one inevitably changes the entanglement length in addition to intercrossability of chains. It is known from previous simulations using Lennard-Jones as well as some coarse-grained models that increasing chain stiffness intensifies reptation [41–43]. To account for this in order to use coarse-grained methods such as DPD with soft potentials in a controlled way, one should use (at least) the persistence length as a measure that should be matched between the coarse-grained and the atomistic models. Here, we did not attempt to do that systematically.

Here, we made no attempt to determine the precise scaling exponents for the diffusion coefficient or the longest relaxation time. In addition, there are a lot of subtleties, such as the tube dimensions, lifetime, friction, and the plateau modules, related to the scaling behavior [11]. A future publication will focus on them and the detailed mechanisms.

Let us next discuss particle density. In many DPD simulations the typical densities have been $\rho=3$ and $\rho=4$, whereas here we have used $\rho=1$. Although our approach as such is not restricted to any particular densities, it worthwhile to discuss this in more detail. Density arises from the coarse-graining process itself, for DPD that has been described in detail, e.g., by Groot [20] while Louis [44] provides a more general discussion. The usual way how DPD particle mapping is defined is by matching compressibilities or solubilities. That provides the interaction parameters. Then, it is typically assumed that each bead contains the same amount of matter. However, although having received little attention thus far, Shillcock *et al.* [45,46] have shown that for a more realistic DPD model of (in their case polyethylene oxide/polyethylethylene, PEO/PEE) block co-polymers, one needs densities that are typically around $\rho=1$ as used here. They also showed that the densities may be slightly different for different types of particles. Importantly, they showed that the typical high densities used in DPD simulations produced unphysical results, in particular for elastic moduli and bulk densities. That implies that for modeling dense polymeric systems, the appropriate densities are likely to be around $\rho=1$ as used here rather than the typical $\rho=4$. In general, the interaction potentials in DPD (and thus also ultimately density) may be more realistically described by density dependent potentials as has been shown by Pagonabarraga and Frenkel [47] and Warren [48]. This discussion also shows our rationale behind choosing $\rho=1$.

Before closing, we would like to discuss briefly the importance of hydrodynamic interactions as it is a closely related issue—the Rouse model does not include hydrodynamics whereas the Zimm theory recognizes the importance of hydrodynamics which is incorporated via the Oseen tensor. As this is fundamentally related to the behavior of polymers in solutions and polymer melts, there has been a long-standing interest in this issue, see, e.g., Refs. [49,50], and references therein. For example, in microphase separation of block co-polymer melts it has been shown that the inclusion of hydrodynamic interactions is critical for obtaining the hexatic phase [51] but the same study also showed that the formation of the lamellar phase is not dependent on hydrodynamics. In another very recent study, Jiang *et al.* [50] focused on how hydrodynamic interactions develop in polymer solutions. Their results are very interesting, but it was still not possible to determine how hydrodynamic interactions develop under different conditions. The importance of

hydrodynamic interactions in polymer solutions remains a field of active research.

Finally, it is important to notice that the approach presented here is not restricted to DPD and the simple linear conservative force in Eq. (1) but can be used at any coarse-graining level if and when needed if interpenetration of particles becomes a problem. That is particularly important in simulations of systems such as lipid bilayers as the bilayer itself is relatively densely packed, and applying, e.g., constant pressure condition (i.e., NpT simulation) may even alter the morphology of the system due to particle overlaps [25,26]. Furthermore, processes such as diffusion cannot be described if particles are able to slide through each other.

ACKNOWLEDGMENTS

This work has been supported by Emil Aaltonen foundation (M.K.), the Academy of Finland through its Center of Excellence Program (I.V.), the Academy of Finland (M.K., I.V.), and the Natural Sciences and Engineering Council of Canada (M.K.). We also thank the Finnish IT Center for Science (CSC), the Southern Ontario SharcNet grid computing facility, the Laboratory of Computational Engineering at Helsinki University of Technology, and the HorseShoe (DCSC) supercluster computing facility at the University of Southern Denmark for computer resources.

[1] S. F. Edwards, Proc. Phys. Soc. London **92**, 9 (1967).
[2] P. G. de Gennes, J. Chem. Phys. **55**, 572 (1971).
[3] M. Doi and S. F. Edwards, *The Theory of Polymer Dynamics* (Clarendon Press, Oxford, 1986).
[4] T. C. B. McLeish, Adv. Phys. **51**, 1379 (2002).
[5] R. Everaers, S. K. Sukumaran, G. S. Grest, C. Svaneborg, A. Sivasubramanian, and K. Kremer, Science **303**, 823 (2004).
[6] S. K. Sukumaran, G. S. Grest, K. Kremer, and R. Everaers, J. Polym. Sci., Part B: Polym. Phys. **43**, 917 (2005).
[7] D. Richter, B. Farago, L. J. Fetters, J. S. Huang, B. Ewen, and C. Lartigue, Phys. Rev. Lett. **64**, 1389 (1990).
[8] J. Käs, H. Strey, and E. Sackmann, Nature (London) **368**, 226 (1994).
[9] P. Schleger, B. Farago, C. Lartigue, A. Kollmar, and D. Richter, Phys. Rev. Lett. **81**, 124 (1998).
[10] K. Kremer, G. S. Grest, and I. Carmesin, Phys. Rev. Lett. **61**, 566 (1988).
[11] M. Pütz, K. Kremer, and G. S. Grest, Europhys. Lett. **49**, 735 (2000).
[12] W. Paul, K. Binder, D. W. Heermann, and K. Kremer, J. Chem. Phys. **95**, 7726 (1991).
[13] J. T. Padding and W. J. Briels, J. Chem. Phys. **115**, 2846 (2001).
[14] W. Paul and G. D. Smith, Rep. Prog. Phys. **67**, 1117 (2004).
[15] H. C. Öttinger, J. Non-Newtonian Fluid Mech. **120**, 207 (2004).
[16] K. Kremer, S. K. Sukumaran, R. Everaers, and G. S. Grest, Comput. Phys. Commun. **169**, 75 (2005).
[17] S. Förster and T. Plantenberg, Angew. Chem., Int. Ed. **41**, 689 (2002).
[18] S. Rastogi, D. R. Lippits, G. W. M. Peters, R. Graf, Y. Yao, and H. W. Spiess, Nat. Mater. **4**, 635 (2005).
[19] P. E. Rouse, J. Chem. Phys. **21**, 1272 (1953).
[20] R. D. Groot, in *Novel Methods in Soft Matter Simulations*, Vol. 640, edited by M. Karttunen, I. Vattulainen, and A. Lukkarinen,Lecture Notes in Physics (Springer-Verlag, Heidelberg, 2004), pp. 5–38.
[21] N. A. Spenley, Europhys. Lett. **49**, 534 (2000).
[22] X. Guerrault, B. Rousseau, and J. Farago, J. Chem. Phys. **121**, 6538 (2004).
[23] J. T. Padding and W. J. Briels, J. Chem. Phys. **117**, 925 (2002).
[24] G. Pan and C. W. Manke, Int. J. Mod. Phys. B **17**, 231 (2003).
[25] A. F. Jakobsen, O. G. Mouritsen, and G. Besold, J. Chem. Phys. **122**, 204901 (2005).
[26] M. P. Allen, J. Phys. Chem. B **110**, 3823 (2006).
[27] P. Español and P. Warren, Europhys. Lett. **30**, 191 (1995).
[28] K. Kremer and F. Müller-Plathe, Mol. Simul. **28**, 729 (2002).
[29] A. P. Lyubartsev, M. Karttunen, I. Vattulainen, and A. Laaksonen, Soft Mater. **1**, 121 (2003).
[30] T. Murtola, E. Falck, M. Patra, M. Karttunen, and I. Vattulainen, J. Chem. Phys. **121**, 9156 (2004).
[31] T. Murtola, T. Rog, E. Falck, M. Karttunen, and I. Vattulainen, Phys. Rev. Lett. **97**, 238102 (2006).
[32] R. D. Groot and P. B. Warren, J. Chem. Phys. **107**, 4423 (1997).
[33] G. S. Grest and K. Kremer, Phys. Rev. A **33**, 3628 (1986).
[34] K. Kremer and G. S. Grest, J. Chem. Phys. **92**, 5057 (1990).
[35] G. Besold, I. Vattulainen, M. Karttunen, and J. M. Polson, Phys. Rev. E **62**, R7611 (2000).
[36] J. C. Shillcock and R. Lipowsky, Nat. Mater. **4**, 225 (2005).
[37] I. Vattulainen, M. Karttunen, G. Besold, and J. M. Polson, J. Chem. Phys. **116**, 3967 (2002).
[38] P. Nikunen, M. Karttunen, and I. Vattulainen, Comput. Phys. Commun. **153**, 407 (2003).
[39] M. Doi, J. Polym. Sci., Polym. Lett. Ed. **19**, 265 (1981).
[40] D. S. Pearson, G. Ver Strate, E. von Meerwall, and F. C. Schilling, Macromolecules **20**, 1133 (1987).
[41] R. Faller, F. Müller-Plathe, and A. Heuer, Macromolecules **33**, 6602 (2000).
[42] R. Faller and F. Müller-Plathe, ChemPhysChem **2**, 180 (2001).
[43] R. Faller and F. Müller-Plathe, Polymer **43**, 621 (2002).
[44] A. A. Louis, J. Phys.: Condens. Matter **14**, 9187 (2002).
[45] V. Ortiz, S. O. Nielsen, D. E. Discher, M. L. Klein, R. Lipowsky, and J. C. Shillcock, J. Phys. Chem. **109**, 17708 (2005).
[46] J. C. Shillcock and R. Lipowsky, J. Phys.: Condens. Matter **18**, S1191 (2006).
[47] I. Pagonabarraga and D. Frenkel, Mol. Simul. **25**, 167 (2000).
[48] P. B. Warren, Phys. Rev. Lett. **87**, 225702 (2001).
[49] P. Ahlrichs, R. Everaers, and B. Dünweg, Phys. Rev. E **64**, 040501(R) (2001).
[50] W. Jiang, J. Huang, Y. Wang, and M. Laradji, J. Chem. Phys. **126**, 044901 (2007).
[51] R. D Groot, T. J. Madden, and D. J. Tildesley, J. Chem. Phys. **110**, 9739 (1999).